

# JGR Atmospheres

## RESEARCH ARTICLE

10.1029/2018JD029775

### Key Points:

- Eight baseflow separation methods were reviewed and applied to evaluate baseflow variations on the Loess Plateau
- Annual baseflow showed a statistically significant downward trend on the Loess Plateau
- Human activity contributed more than 73% to average baseflow decline

### Supporting Information:

- Supporting Information S1

### Correspondence to:

C. Miao,  
miaocy@vip.sina.com

### Citation:

Wu, J., Miao, C., Duan, Q., Lei, X., Li, X., & Li, H. (2019). Dynamics and attributions of baseflow in the semiarid Loess Plateau. *Journal of Geophysical Research: Atmospheres*, 124, 3684–3701. <https://doi.org/10.1029/2018JD029775>

Received 6 OCT 2018

Accepted 10 MAR 2019

Accepted article online 18 MAR 2019

Published online 2 APR 2019

### Author Contributions:

**Conceptualization:** Jingwen Wu, Xiaoyan Li, Hu Li

**Data curation:** Jingwen Wu, Xiaohui Lei, Xiaoyan Li, Hu Li

**Formal analysis:** Jingwen Wu, Qingyun Duan, Xiaohui Lei

**Methodology:** Jingwen Wu, Xiaoyan Li, Hu Li

**Supervision:** Qingyun Duan

**Writing - original draft:** Jingwen Wu

**Writing - review & editing:** Jingwen Wu, Qingyun Duan, Xiaoyan Li

## Dynamics and Attributions of Baseflow in the Semiarid Loess Plateau

Jingwen Wu<sup>1</sup>, Chiyuan Miao<sup>1</sup> , Qingyun Duan<sup>1</sup> , Xiaohui Lei<sup>2</sup>, Xiaoyan Li<sup>1</sup> , and Hu Li<sup>3</sup>

<sup>1</sup>State Key Laboratory of Earth Surface Processes and Resource Ecology, Faculty of Geographical Science, Beijing Normal University, Beijing, China, <sup>2</sup>State Key Laboratory of Simulation and Regulation of Water Cycle in River Basin, China Institute of Water Resources and Hydropower Research, Beijing, China, <sup>3</sup>Key Laboratory of Agricultural Non-point Source Pollution Control, Ministry of Agriculture/Institute of Agricultural Resources and Regional Planning, Chinese Academy of Agricultural Sciences, Beijing, China

**Abstract** Baseflow is an all-important replenishment feature of the hydrologic cycle for maintaining surface water in basins across the world. Understanding its dynamics and the influence of climate variability and human activities will be beneficial for developing sustainable water-management strategies. In this study, we selected 11 basins within the Loess Plateau (a typical semiarid region in China) for assessment of the variations in baseflow and baseflow index (*BFI*; the ratio of baseflow volume to total streamflow volume) during the period 1961–2014. We compared eight baseflow separation methods and selected the median series in order to reduce the uncertainty. Results showed that values of the “Bflow” and Eckhardt filter methods were higher than values of the other six methods for the period of peak discharge. Annual baseflow exhibited a statistically significant downward trend ( $p < 0.01$ ) in all 11 basins except Qingjian and Yanhe basins, while nine basins trended upward for *BFI*. All basins exhibited downward trends for seasonal baseflow in all seasons, with Yanhe and Qingjian showing the least significant trend. Variations in both baseflow and the *BFI* were more sensitive to variations in potential evapotranspiration than to variations in precipitation. Across these 11 basins for both the conservation engineering period (1971–1999) and the reforestation period (2000–2014), human activities (73% and 76%, respectively) contributed more than climate variability (27% and 24%, respectively) to average baseflow decline. However, climate variability was the main factor altering the *BFI*, with the contribution accounting for about 54% and 76%, respectively, for the two periods.

## 1. Introduction

Baseflow is the perennial flow portion of streamflow. In previous studies, the terminology usage is inconsistent, with *baseflow*, *low flow*, and *drought flow* commonly used interchangeably to denote either the streamflow resulting from sustained subsurface inputs to the stream channel or the lowest annual streamflow within a watershed or region (Price, 2011). In this study, baseflow is generally used to denote streamflow fed from deep groundwater and from delayed shallow subsurface storage during and following precipitation and snowmelt events. It is the interconnection between groundwater and surface water and plays an important role in the health of river ecosystems (Ficklin et al., 2016). The quantity and quality of baseflow discharged to streams are influenced by a combination of climate and basin characteristics. Over the past century, rising global temperatures have led to a more energized hydrologic cycle, particularly in semiarid regions due to the fragile nature of their eco-hydrology (Seager et al., 2010; Yang, Jia, et al., 2019). Semiarid regions cover about 15% of the Earth's land surface and support about 20% of the global population (Huang et al., 2016); however, the water resources of these semiarid regions account for less than 2% of the global total (Standish-Lee et al., 2005). In these water-limited areas, surface water flows are mainly supplied by baseflow, making baseflow an extremely important low-flow hydrologic characteristic. Therefore, understanding and quantifying the dynamic variations and contributions of baseflow to streamflow are critical for ensuring appropriate water resource management (especially for drought conditions) and environmental protection.

Baseflow is difficult to measure directly compared with surface runoff. Numerous baseflow separation approaches have been developed in order to quantify the baseflow, including hydrograph separation (HYSEP; e.g., slash separation method and recession curve analysis; Linsley et al., 1975; Tallaksen, 1995),

numerical simulation (e.g., smoothed minima, HYSEP, and digital filtering methods; Nathan & McMahon, 1990), water balance (e.g., reservoir assumption and parameter separation methods; Harman & Sivapalan, 2009), and chemical mass balance HYSEP (Tetzlaff & Soulsby, 2008). Numerical simulations are currently the most widely used methods to quantify baseflow, because the models are easy to operate, can avoid the subjectivity and arbitrariness of a manual separation method, and are suitable for long-term hydrologic series (Xu et al., 2016). Mwakalila et al. (2002) used the baseflow index (*BFI*) method to examine the influence of physical catchment properties on baseflow in these water-limited environments; they showed that the *BFI*, which is the ratio of baseflow volume to total streamflow volume, has a strong relationship with the drainage density index. Ficklin et al. (2016) used the HYSEP method to separate baseflow and to characterize the impacts of climatic change on trends in baseflow and stormflow in watersheds of the United States; consistent trends in baseflow and stormflow were found, with increases during the fall and winter in the northeast and decreases during all seasons in the southwest. Fan et al. (2013) applied digital filtering to separate baseflow from streamflow and then to investigate the dynamics of baseflow in four headstreams of the Tarim River Basin, China, from 1960 to 2007; the baseflow appeared to show obvious seasonal variation, the lowest baseflow mainly occurring in winter and the largest baseflow in summer.

With increasing awareness of the importance of baseflow to stream dynamics, more research has focused on baseflow response to climate variability and human activities (Ahiablame et al., 2017; Juckem et al., 2008; Li, Liu, & Zhang, 2018). Baseflow is an important replenishment resource for maintaining surface water in semiarid areas. Understanding the individual effects that climate variability and human activities have on changes in baseflow in these water-limited semiarid basins will be beneficial for developing sustainable water-management strategies and providing a dependable water source for food production.

Xu et al. (2013) used climate elasticity and the residual method to assess the relative importance of climate and land surface changes on baseflow variations at 55 unregulated watersheds in the Midwest of the United States. Baseflow was found to have increased in 58% of watersheds, and land surface change contributed 2.7 times more to baseflow than climate change ( $74\% \pm 10\%$  vs.  $27\% \pm 10\%$ , respectively). Christine et al. (2015) used the conductivity mass balance in the Upper Colorado River Basin and showed that baseflow was positively correlated with precipitation, land surface slope, sandy soils content, and some land cover characteristics, while Zomlot et al. (2015) used the digital filter method to show that variation in vegetation cover was the main driver of the large spatial variation in baseflow in the northern part of Belgium.

However, most previous studies have only qualitatively analyzed the effects of climate variability and human activities on baseflow variation; quantitative attributions of baseflow variation at the basin scale remain rare, especially for semiarid basins. In addition, most previous studies generally employ only one method to separate baseflow from streamflow, and this may lead to uncertainty within the final results. Because the true values of baseflow are unknown, the method that gives the best estimates remains undetermined (Eckhardt, 2008). Thus, multiple baseflow separation methods should be used simultaneously to reduce the uncertainty of the results.

The Loess Plateau in China is a typical semiarid region with little precipitation and high potential evapotranspiration. It has been an important agricultural region in China for thousands of years and currently supports 114 million people or 8.5% of the country's total population (Kong et al., 2016). During the last several decades, the Loess Plateau has undergone persistent climate warming and intensified human activities. In particular, the *Grain for Green* program, implemented in 1999, and large-scale reforestation programs have led to obvious transformations of regional land use and land cover. Consequently, the ongoing downward trend in streamflow in this region has been significant (Wu et al., 2017).

Previous studies in the region have mainly focused on the decline in surface runoff (Gao et al., 2016; Hu et al., 2017; Liang et al., 2015), whereas research studies on the analysis and causes of baseflow variation are rare. Therefore, the main objectives of this study are to (1) fully document regional patterns and variation of baseflow based on multiple baseflow separation methods in 11 catchments of the Loess Plateau and (2) quantify the relative influence of climate variability and human activities on baseflow. Our study is designed to fill the gaps in our knowledge of baseflow variation and the causes of its variation within the Loess Plateau. Our findings will contribute to the development of scientific water-resource management strategies and the restoration of the ecological balance of the Loess Plateau and at the same time provide a deeper understanding of the hydrologic processes in semiarid basins.

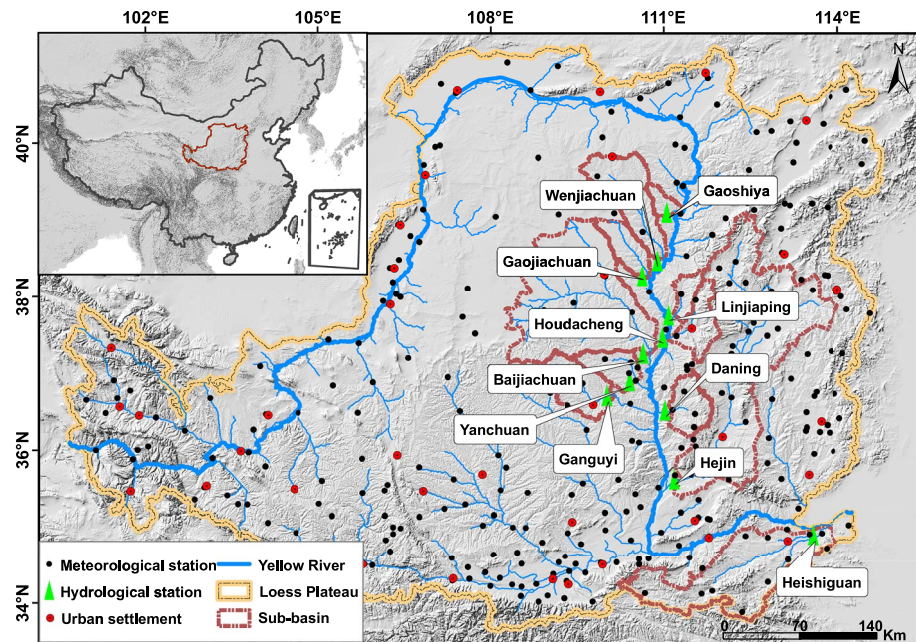


Figure 1. Geographic location of the 11 basins and respective hydro-meteorological stations.

## 2. Study Area and Data Source

The Loess Plateau (35–41°N, 102–114°E) is located in the upper-middle reaches of the Yellow River in north-west China (Figure 1). It covers an area of about 640,000 km<sup>2</sup>, accounting for 6.6% of the total area of China (Fu et al., 2011). The plateau is a typical semiarid region that is influenced by high-intensity monsoon activity. The average annual temperature is approximately 9.0 °C, and the average annual precipitation is about 420 mm, which mainly falls from June to September (i.e., 60–70% of the total precipitation) in high-intensity storms. Due to the area’s unique climatic features and increasingly intense human activities over the last five decades, the streamflow has displayed a significant downward trend (Wu et al., 2017) and has resulted in the area becoming one of the most water-limited regions in China. In this study, we selected 11 primary basins located in semiarid regions of the Loess Plateau that have strong climatic and land-surface gradients; these features were chosen to represent the combined effects of climatic and land-surface factors. Details of these 11 basins and the long-term hydro-meteorological variables are shown in Table 1.

Daily streamflow data were collected from 1961 to 2014 for 11 hydrologic stations within the Loess Plateau by the Yellow River Conservancy Commission. Daily precipitation and daily minimum and maximum

**Table 1**

*Detailed Summary of the Hydrological Variables Associated With the 11 Loess Plateau Basins During the Period 1961–2014*

Acronym	Basin	Hydrologic station	Area (km <sup>2</sup> )	P (mm)	E (mm)	Q (mm)
GSC	Gushanchuan	Gaoshiya	1,263	425.8	1,038.1	47.05
KY	Kuye	Wenjiachuan	8,515	400	1,006.1	57.85
TW	Tuwei	Gaojiachuan	3,253	405.1	1,013.9	95.12
WD	Wuding	Baijiachuan	29,662	379	1,047.4	36.1
QJ	Qingjian	Yanchuan	3,468	506.8	1,040.7	38.31
YH	Yanhe	Ganguyi	5,891	541.9	1,100.6	33.91
YL	Yiluo	Heishiguan	18,563	716	1,055.6	126.28
QS	Qiushui	Linjiaping	1,873	442.8	1,170.8	32.34
SC	Sanchuan	Houdacheng	4,104	553.1	962.2	50.51
FH	Fenhe	Hejin	38,728	512	1,059.4	21.99
XS	Xinshui	Danling	3,992	575.7	992.6	28.84

Note. P, E, and Q denote the annual mean precipitation, annual mean potential evapotranspiration, and annual mean streamflow, respectively.

temperatures in the same time period were obtained from the China Meteorological Data Sharing Service System (<http://data.cma.cn>). Potential evapotranspiration was calculated by the Hargreaves and Samani method (Hargreaves & Samani, 1985). Nearest neighbor interpolation and ArcMap software were used to generate spatially averaged meteorological data across the entire study area.

### 3. Methodology

#### 3.1. Baseflow Separation

A number of numerical simulation baseflow-separation methods have been developed to estimate the baseflow of streamflow. Although each of the methods is based on formalized algorithms for separating the baseflow component of streamflow, the methods are subjective and not based on mathematical solutions to groundwater-flow or overland-flow equations. As a consequence, it is beneficial to use more than one baseflow separation method to analyze a streamflow record and then to compare the results of the different methods. The U.S. Geological Survey (USGS) Groundwater Toolbox, which incorporates eight widely used baseflow separation methods (Barlow et al., 2017), has been used to separate baseflow from total streamflow (Ficklin et al., 2016; Partington et al., 2012). These methods include the Base-Flow Index (*BFI*; standard and modified; Nathan & McMahon, 1990; Wahl & Wahl, 1995), HYSEP (fixed interval, sliding interval, and local minimum; Sloto & Crouse, 1996), PART method (Rutledge, 1998), the Soil and Water Assessment Tool (SWAT) *Bflow* method (Arnold & Allen, 1999), and Eckhardt filter approaches (Eckhardt, 2005). The algorithm details of each baseflow separation method are as follows:

##### 3.1.1. *BFI* method

The *BFI* program (Wahl & Wahl, 1995) is based on a series of procedures developed by the Institute of Hydrology and mimics two separation methods (i.e., the *BFI*-standard method and *BFI*-modified method). It first partitions daily streamflow into intervals of length in  $N$  days. The minimum daily streamflow during each  $N$ -day interval is then identified and compared to adjacent minima to determine *turning points*. If the minimum is multiplied by 0.9 (a turning point test factor that has no physical meaning) and is less than both adjacent minima, then that minimum is a turning point. The baseflow hydrograph is then identified by connecting these turning points. In the *BFI*-modified method, parameter  $f$  is replaced by a daily recession index  $K$ , and the turning point test considers the actual number of days between turning point candidates.

##### 3.1.2. HYSEP method

HYSEP is an automated baseflow separation computer program that mimics three separation methods (i.e., fixed interval, sliding interval, and local minimum). The three methods use different algorithms to determine the baseflow hydrograph between low points of the streamflow hydrograph. Surface runoff duration is estimated from the empirical relation:

$$N = A^{0.2}, \quad (1)$$

where  $N$  is the duration after which surface runoff ceases and  $A$  is the drainage area. The odd integer between 3 and 11 nearest to  $2N$  is selected as the interval to estimate the baseflow. In the fixed-interval method, the daily streamflow hydrograph is partitioned into nonintersecting intervals. The minimum discharge in each interval is assigned to describe the baseflow over the entire interval. The sliding-interval method finds the lowest discharge in one-half the interval minus 1 day. The local-minimum method detects each day to determine if it is the lowest discharge in one-half the interval minus 1 day. If it is, then it is a local minimum and is connected by straight lines to adjacent local minima.

##### 3.1.3. PART method

PART is a streamflow partitioning program developed by the USGS to estimate daily baseflow (Rutledge, 1998). It implements a characteristic response time in days, similar to the HYSEP method, which is a function of the drainage area of the basin (equation (1)). If daily streamflow values decrease for  $N$  or more days, then the requirement of antecedent recession is met and it is assumed that baseflow is equal to streamflow for these days. In addition, it performs a linear interpolation between each day in the record that meets this requirement. However, the baseflow obtained by linear interpolation may be greater than the total streamflow, and thus, an error check is needed to ensure that baseflow never exceeds streamflow. The criterion for streamflow to meet the antecedent recession requirement is that streamflow never decreases by more than 0.1 log cycle on days.

### 3.1.4. The SWAT Bflow method

The Bflow program (Arnold & Allen, 1999) uses a method first proposed by Lyne and Hollick (1979). This technique has no true physical basis; it is objective and reproducible. The equation of the filter is expressed as

$$q_t = \beta q_{t-1} + \frac{1 + \beta}{2} (Q_t - Q_{t-1}). \quad (2)$$

where  $q_t$  is the filtered surface runoff at the  $t$  time step,  $Q_t$  is the total streamflow, and  $\beta$  is the filter parameter (0.925). The default value of 0.925 was determined by Nathan and McMahon (1990). Thus, baseflow  $b_t$  is estimated as

$$b_t = Q_t - q_t. \quad (3)$$

The filter is passed over the streamflow data three times (forward, backward, and forward), and in this study, we used the result based on the first pass (forward).

### 3.1.5. Eckhardt filter method

The Eckhardt filter is a two-parameter filter based on the assumption that aquifer outflow is linearly proportional to storage. The method limits the maximum ratio of baseflow to streamflow and considers runoff to be a nonnegligible low-frequency component. The runoff component was initially proposed by Spongberg (2000) and later supported by Eckhardt (2005), who described this as potentially beneficial. The equation for this filter is expressed by Eckhardt (2005) as

$$b_t = \frac{(1 - BFI_{\max}) a b_{t-1} + (1 - a) BFI_{\max} Q_t}{1 - a BFI_{\max}}, \quad (4)$$

where  $BFI_{\max}$  is the maximum value of the  $BFI$  and  $a$  is the baseflow recession constant. Previous studies have generally used values ranging from 0.925 to 0.95 for  $a$  (Zhou et al., 2017); in this study, we used a value of 0.925. Eckhardt (2005) suggests using a value of  $BFI_{\max} = 0.80$  for perennial streams with porous aquifers, 0.50 for ephemeral streams with porous aquifers, and 0.25 for perennial streams with hard rock aquifers.

In this study, we first calculated the baseflow using eight methods based on these five types and then used the median of the values calculated by these eight methods to indicate the baseflow. The  $BFI$  was calculated as follows:

$$BFI = \frac{\text{Baseflow}}{\text{Streamflow}}, \quad (5)$$

## 3.2. Attribution Analysis of Baseflow

The concept of elasticity (Schaake, 1990) has been used to evaluate the sensitivity of runoff to changes in climate. In this study, we used the elasticity approach to quantify the relative contributions of climate variability and human activities to changes in baseflow. The climate elasticity of baseflow ( $\epsilon$ ) is defined as the ratio of the baseflow variation (or  $BFI$ ) rate to the variation rate of a certain climate factor ( $X$ , precipitation or potential evapotranspiration in this study) and is expressed as

$$\epsilon = \frac{\partial Q_b / Q_b}{\partial X / X}, \quad (6)$$

where  $\epsilon$  indicates the climate elasticity of baseflow,  $Q_b$  indicates baseflow (or  $BFI$ ), and  $X$  indicates precipitation or potential evapotranspiration.

We used the least squares estimator to estimate climate elasticity of the annual baseflow (Zheng et al., 2009); this is expressed as

$$\epsilon = \frac{\bar{X}}{Q_b} \sum (X_i - \bar{X}) \left( \frac{(Q_{bi} - \bar{Q}_b)}{\sum (X_i - \bar{X})^2} \right) = \frac{\rho_{XQ} C_Q}{C_X}, \quad (7)$$

where  $Q_b$  is annual baseflow (or  $BFI$ ),  $X$  is the annual climate variables (precipitation and potential

evapotranspiration in this study),  $\bar{X}$  and  $\bar{Q}$  are the multiyear annual mean climate variables and baseflow values (or *BFI*), respectively,  $\rho_{XQ}$  is the correlation coefficient between climate variables and baseflow (or *BFI*), and  $C_X$  and  $C_Q$  are coefficients of variation in climate variables and baseflow (or *BFI*), respectively. To evaluate the relative contributions of climate variability and human activities on baseflow variation (or *BFI*), the following steps were performed:

1. Calculation of climate elasticity  $\varepsilon$ . Based on the baseflow (or *BFI*) data for the entire period of record and equation (7), climate elasticity ( $\varepsilon$ ) with respect to precipitation ( $\varepsilon_P$ ) and potential evapotranspiration ( $\varepsilon_{E_0}$ ) was calculated for baseflow (or *BFI*).
2. Determination of a baseline period. Based on our previous work (Wu et al., 2017), the *human-designated* method was used to determine the baseline period, for which the anthropogenic influence was assumed to be weaker during a preselected earlier period of time. Thus, in this study, the period 1961–1970 was selected as the baseline period (Miao et al., 2011; Zhang et al., 2016). Next, based on the development of soil and water conservation measures across the Loess Plateau, the period 1971–1999 was designated the *conservation engineering period* during which many soil and water conservation engineering projects were implemented (Gao et al., 2016; Zhang et al., 2011). The Grain for Green program was implemented after 1999, and the period 2000–2014 was designated the *reforestation period* (Fu et al., 2017).
3. Based on equation (6), the climate-induced baseflow (or *BFI*) variation in the conservation engineering period (or reforestation period) relative to the baseline period was calculated as follows:

$$\Delta\bar{Q}_b^{\text{climate}} = (\varepsilon_P \Delta P / P + \varepsilon_{E_0} \Delta E_0 / E_0) Q_b, \quad (8)$$

where  $\Delta\bar{Q}_b^{\text{climate}}$  is the change in the annual mean baseflow (or *BFI*) caused by climate variability;  $\Delta P$  and  $\Delta E_0$  are changes in precipitation and potential evapotranspiration, respectively; and  $P$ ,  $E_0$ , and  $Q_b$  are long-term mean values of precipitation, potential evapotranspiration, and baseflow (or *BFI*) during the baseline period, respectively. Therefore, the change in the annual mean baseflow (or *BFI*) caused by human activities ( $\Delta\bar{Q}_b^{\text{human}}$ ) can be calculated as

$$\Delta\bar{Q}_b^{\text{human}} = \Delta Q_b - \Delta\bar{Q}_b^{\text{climate}} \quad (9)$$

where  $\Delta Q_b$  indicates the change in baseflow (or *BFI*). Thus, the percentage contribution of climate-induced ( $P_c$ ) and human-activity-induced ( $P_h$ ) baseflow (or *BFI*) changes can be calculated as follows:

$$P_c = \frac{\Delta\bar{Q}_b^{\text{climate}}}{|\Delta\bar{Q}_b^{\text{climate}}| + |\Delta\bar{Q}_b^{\text{human}}|} \times 100\% \quad \text{and} \quad P_h = \frac{\Delta\bar{Q}_b^{\text{human}}}{|\Delta\bar{Q}_b^{\text{climate}}| + |\Delta\bar{Q}_b^{\text{human}}|} \times 100\%, \quad (10)$$

### 3.3. Estimation of the Dynamic $n$ at the Catchment Scale

Determination of dynamic (temporally changing)  $n$  in Budyko-based Choudhury equation ( $\frac{E}{P} = \frac{E_0/P}{(1+(E_0/P)^n)^{1/n}}$ ; Choudhury, 1999) which is popularly used in studies of the Loess Plateau (Liang et al., 2015; Liu et al., 2017), is very important and greatly affects the applicability of Budyko hypothesis (Budyko, 1974). Parameter  $n$  in Choudhury equation represents the interactions between climate and land surface properties. Variations in climate (e.g., seasonality and storm) and basin characteristics (e.g., slope, land use change, and engineering construction), which play important roles in water energy balance (Berghuijs et al., 2017; Liang et al., 2015), could cause temporal changes in  $n$ . Therefore, using dynamic (temporally changing)  $n$ , could reflect changing interactions between climate and basin characteristics. In the original Budyko framework, which was deduced for long time scales, and water storage changes can be negligible based on the water balance equation (Yang et al., 2008; Zhou et al., 2015). However, for shorter periods, water storage change becomes important in the water balance. Thus, Choudhury equation can be rewritten as

$$\frac{E}{P-\Delta S} = \frac{E_0/(P-\Delta S)}{(1+(\frac{E_0}{P-\Delta S})^n)^{1/n}} \quad (11)$$

where  $\Delta S$  denotes the water storage change. At present, long-term  $\Delta S$  data are not regularly available. In this

case, we use a relatively prolonged moving windows approach (5 years) to calculate the dynamic  $n$  at the basin scale, and thus,  $\Delta S$  could be negligible compared to other hydrologic variables (i.e., precipitation, potential evapotranspiration, and runoff). The parameter  $n$  at year 1963 was calculated using mean annual precipitation, potential evapotranspiration, and runoff during the period 1961–1965; the parameter  $n$  at year 1964 was calculated using the mean annual precipitation, potential evapotranspiration, and runoff during the period 1962–1966. Therefore, with a 54-year coverage of the input data (1961–2014), a total of 50  $n$  values (1963–2012) could be obtained.

### 3.4. Statistical Analyses

The Mann-Kendall nonparametric trend test (Kendall, 1975) was used to detect trends and trend significance of hydro-climatologic variables at annual and seasonal scales from 1961 to 2014 (spring, March to May; summer, June to August; autumn, September to November; and winter, December to February). The autocorrelation in the time series was first removed based on the methods proposed by Yue et al. (2002). The detailed process can be found in Wu, Miao, Tang, et al. (2018) and Wu, Miao, Zheng, et al. (2018). Positive values of the Mann-Kendall statistic  $Z$  indicate an upward trend over time, whereas negative values indicate a downward trend. We considered trends with  $p < 0.05$  as significant at the 95% confidence level and trends with  $p < 0.01$  as significant at the 99% confidence level.

## 4. Results and Discussion

### 4.1. Baseflow Separation

Comparisons of eight baseflow separation methods and the median series at monthly and annual scales for 11 basins on the Loess Plateau from 1961 to 2014 are shown in Figure 2. At both the monthly scale and annual scale, the results of eight baseflow separation methods were generally consistent, especially in the Tuwei, Yiluo, Sanchuan, and Fenhe basins where the streamflow was high compared to other basins on the Loess Plateau and for all basins during the low-flow period. However, peak maxima and duration for Bflow and Eckhardt filter methods were higher than the other methods in the basin without ample streamflow (Gushanchuan, Kuye, Wuding, Qingjian, Yanhe, and Qiushui). We suggest that in the semiarid basins with a lower runoff coefficient, many short-duration high-intensity precipitation events lead to a runoff yield that is mostly excess infiltration that does not extend to the groundwater (i.e., lower groundwater runoff coefficient), and the flood hydrograph is fine lines with short duration (Xu et al., 2011). For all baseflow separation methods used in this study except Bflow and Eckhardt filter methods, determined the baseflow based on the minimum streamflow within fixed time slots. Overall, compared the different separation principle, special climatic conditions, and geological conditions, the baseflow based on these two methods (i.e., Bflow and Eckhardt filter methods) could be greater compared to the other methods in the high-flow season. In order to reduce the uncertainty in the period of peak value in these eight baseflow separation methods, the median series of these eight methods was selected as the dependable baseflow value.

### 4.2. Temporal-Spatial Variations in Baseflow and BFI

#### 4.2.1. Variations in Baseflow at Various Time Scales

Seasonal and annual temporal-spatial baseflow variations during the period 1961–2014 are presented in Figure 3 and Table 2. Mann-Kendall trend analysis of annual baseflow showed a statistically significant downward trend ( $p < 0.01$ ) in all 11 basins except Qingjian ( $Z = 0.54$ ) and Yanhe ( $Z = -0.34$ ), with the greatest downward trend in Tuwei ( $Z = -7.9$ ). The annual mean baseflow storage varied among the 11 basins, with the highest average baseflow storage in Yiluo (5.95) and the lowest in Qiushui (0.85). In addition, the annual mean baseflow storage was, in general, greatest during the period 1961–1970 and lowest between 2001 and 2014 (Figure 4). Several factors have most likely contributed to the low levels seen since 2001. Over the last five decades, potential evapotranspiration has increasingly trended upward on the Loess Plateau (Wu et al., 2017). In addition, although precipitation has not significantly declined, extreme precipitation events have significantly increased (Sun et al., 2015). Because the Loess Plateau typically experiences runoff being generated over the infiltration area (Liu et al., 2012), with the increase in extreme precipitation events, less water has infiltrated into deep soil (Yang, Wang, et al., 2019), leading to lower baseflow storage. Furthermore, with intensifying human activities, water demand and depletion have increased and groundwater levels have decreased. This combination of events led to the smallest annual mean baseflow storage from 2001 to 2014. For the seasonal baseflow, most basins exhibited significant ( $p < 0.05$  or  $p < 0.01$ )

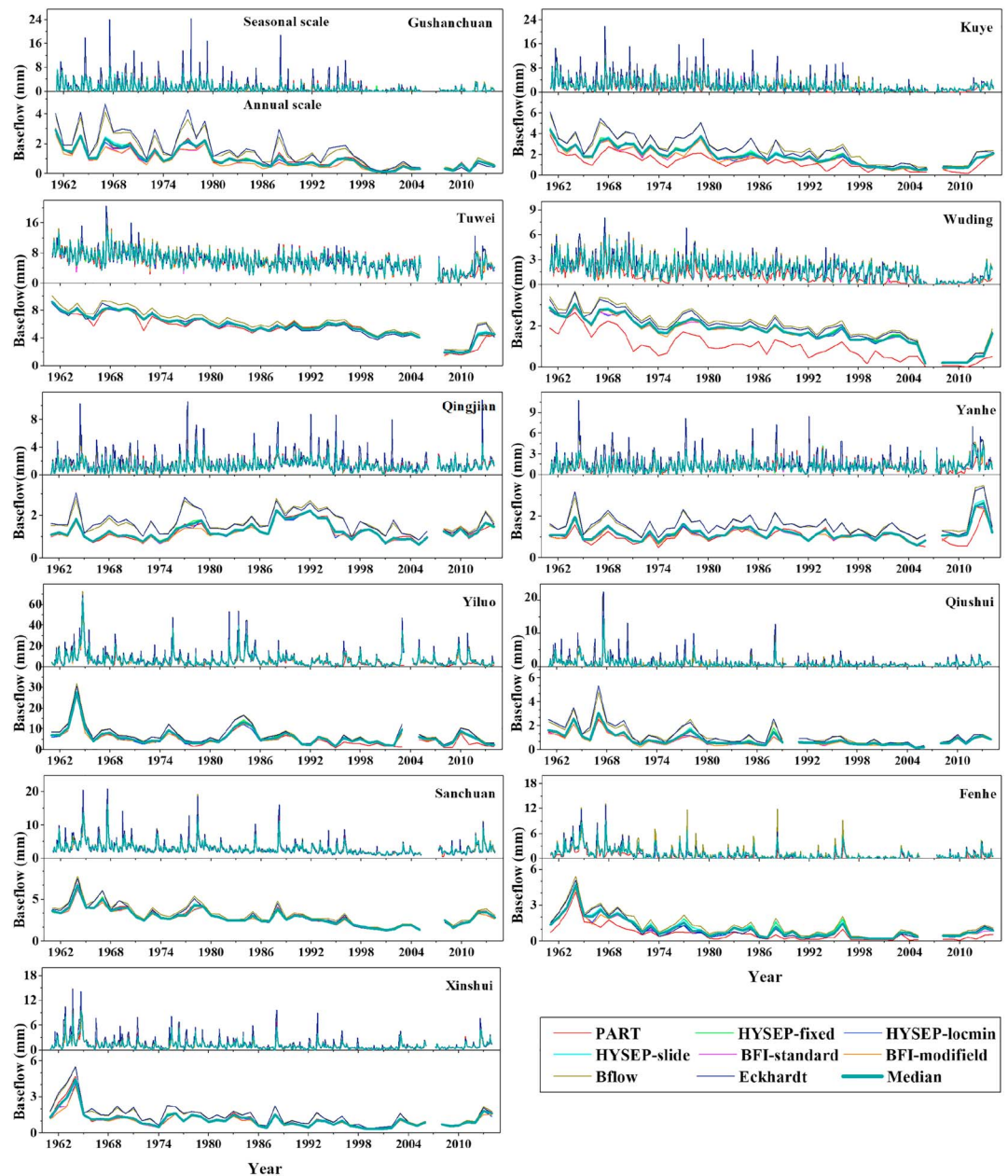


**Figure 2.** Comparison of eight baseflow separation methods and the median series at seasonal (upper) and annual (lower) scales in 11 basins on the Loess Plateau during the period 1961–2014.

downward trends in all seasons (Figure 3). In contrast, Yanhe and Qingjian basins showed insignificant changes during spring and autumn and an increasing trend in summer (Figure 3b) and winter (Figure 3d). In general, baseflow storage was greater in autumn and spring for almost all basins (Table 2).

We also investigated the long-term monthly baseflow storage from 1961 to 2014 (Figure 5) and identified a bimodal trend in the baseflow for all basins except Yiluo and Fenhe, with one peak value in March and one peak value in October (or September). The second peak baseflow value undoubtedly results from the precipitation primarily occurring between June and September (Figure 5) that eventually (by October) becomes part of the baseflow. Baseflow is derived from the drainage of near-surface valley soils and riparian zones, and water concentrates in these areas during and following precipitation events (Brutsaert, 2005). Furthermore, precipitation can seep into the soil to replenish shallow unsaturated storage and then

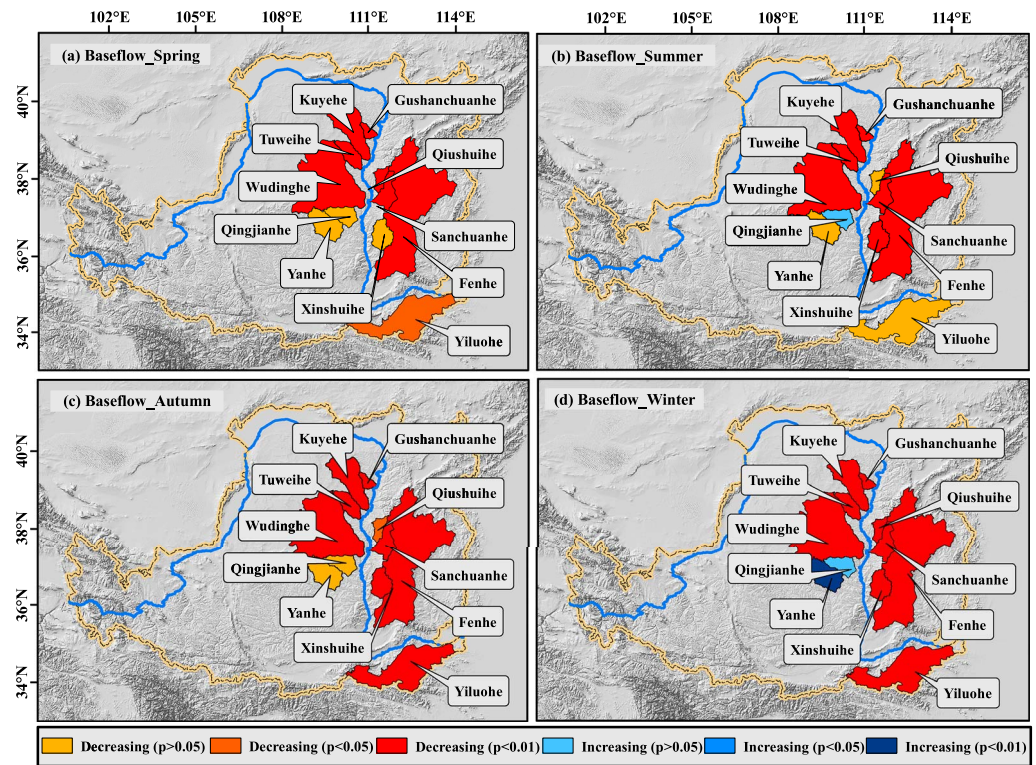


**Figure 3.** Spatial patterns of the Mann-Kendall trend test for seasonal baseflow in 11 basins of the Loess Plateau during the period 1961–2014.

sustain the river channel transmitted from it (Ward & Robinson, 1990). We suggest that the March peak is mainly due to snowmelt because most precipitation during the winter falls as snow, which becomes snowmelt as temperatures rise in late winter/early spring (Wang et al., 2013). In addition, during this part of the year, the demand for irrigation is low and evapotranspiration is relatively weak, which both lead to relatively low water consumption. However, for the Yiluo and Fenhe basins, which did not have a peak in March, we suggest that temperature and land use are the major reasons for the lack of a March peak. As shown in Figure S2 in the supporting information, the average monthly temperature in winter was around 0 °C in the Yiluo basin, the highest value across all basins on the Loess Plateau. Furthermore,

**Table 2**  
*Mann-Kendall Test and Multiyear Average Baseflow at Seasonal and Annual Scales for 11 Basins of the Loess Plateau During 1961–2014*

Basin	Baseflow Z value					Mean baseflow (mm)				
	MAM	JJA	SON	DJF	Annual	MAM	JJA	SON	DJF	Annual
GSC	-7.39**	-3.32**	-4.77**	-3.01**	-6.23**	1.5	0.82	1.36	0.3	1
KY	-6.91**	-4.43**	-5.36**	-4.01**	-6.38**	2.4	1.11	2.56	1.28	1.84
TW	-7.27*	-7.16*	-7.03*	-4.36*	-7.9**	6.3	4.47	6.7	5.67	5.78
WD	-7.63**	-6.33**	-6.55**	-4.68**	-7.72**	1.87	0.97	2.15	1.8	1.7
QJ	-0.87	1.4	-0.13	1.5	0.54	1.37	1.07	1.66	0.95	1.27
YH	-0.22	-0.73	-1.32	4.56**	-0.34	1.35	0.89	1.55	0.89	1.17
YL	-2.1*	-1.39	-3.26**	-3.1**	-2.82**	4.27	5.87	9	4.65	5.95
QS	-3.93**	-1.57	-2.4*	-3.27**	-3.68**	0.75	0.81	1.26	0.56	0.85
SC	-5.28**	-4**	-4.83**	-5.37**	-5.45**	2.55	2.91	3.71	2.32	2.87
FH	-3.99**	-3.13**	-4.3**	-5.67**	-5.02**	0.52	0.93	1.66	0.92	1.01
XS	-1.86	-3.14**	-2.90**	-2.95**	-3.65**	0.87	1.01	1.69	1	1.09

*Note.* March–April–May (MAM), June–July–August (JJA), September–October–November (SON), and December–January–February (DJF) are spring, summer, autumn, and winter, respectively. Basin acronyms are listed in Table 1. BFI, baseflow index.

\*\*Significance at the 99% level. \*Significance at the 95% level.

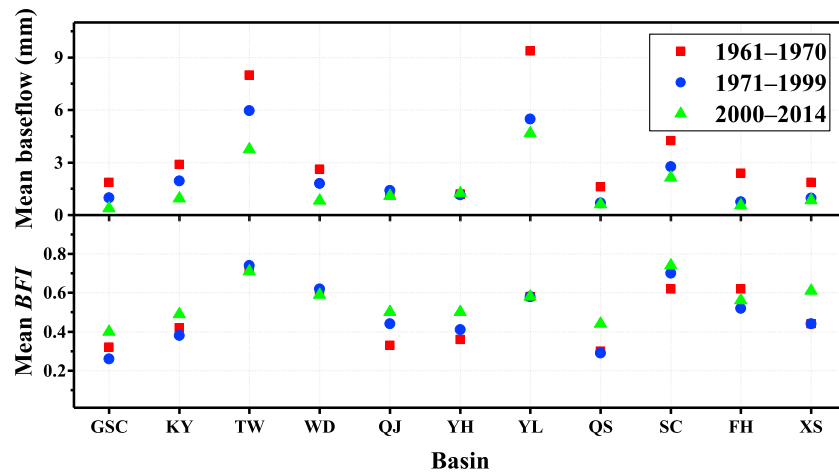


**Figure 4.** Annual mean baseflow and baseflow index (*BFI*) from 1961 to 2014 in 11 basins of the Loess Plateau. Acronyms on the x axis are listed in Table 1.

Wu, Miao, Tang, et al. (2018) and Wu, Miao, Zheng, et al. (2018) showed that the area of farmland is much higher in the Yiluo and Fenhe basins than in other basins, with the main crops being winter wheat and spring corn (Li, Wei, et al., 2018). Thus, more water is needed for crop irrigation at this time of year in these basins, leading to lower baseflow during this period.

**4.2.2. Variations in *BFI* at Various Time Scales**

The temporal-spatial analysis of seasonal and annual *BFI* variation from the 1961 to 2014 is presented in Figure 6 and Table 3. Upward trends were identified in nine basins, with Qingjian ( $Z = 3.95$ ) showing the

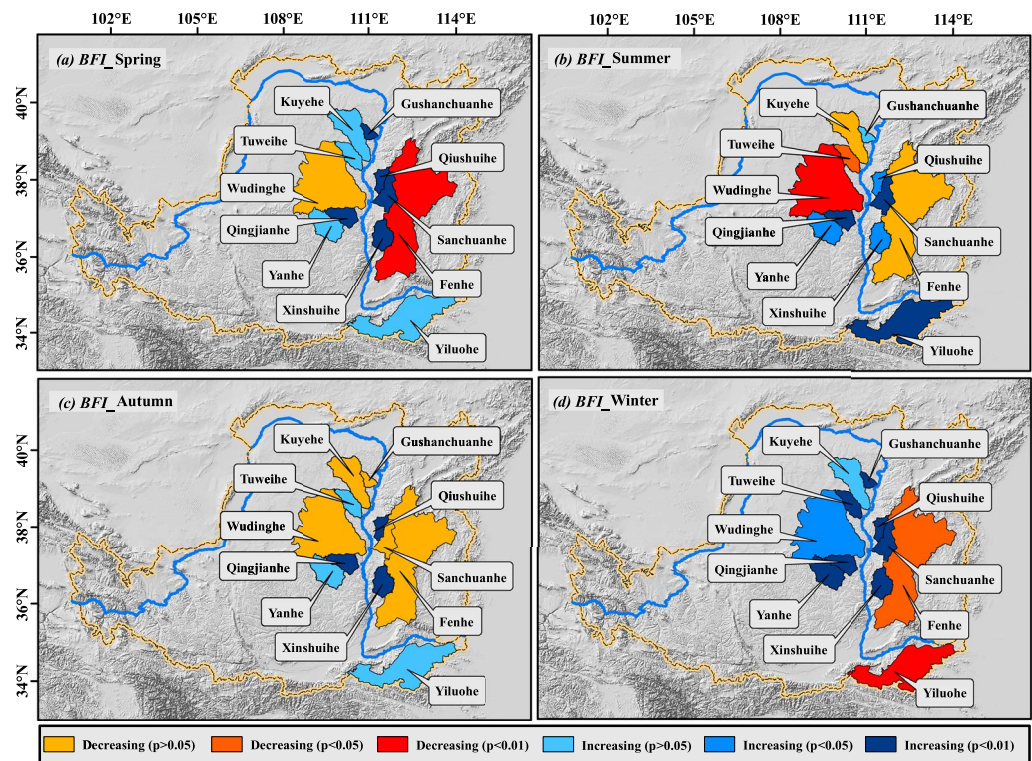


**Figure 5.** Multiannual monthly average precipitation and baseflow in 11 basins of the Loess Plateau during the period 1961–2014. Acronyms are listed in Table 1.

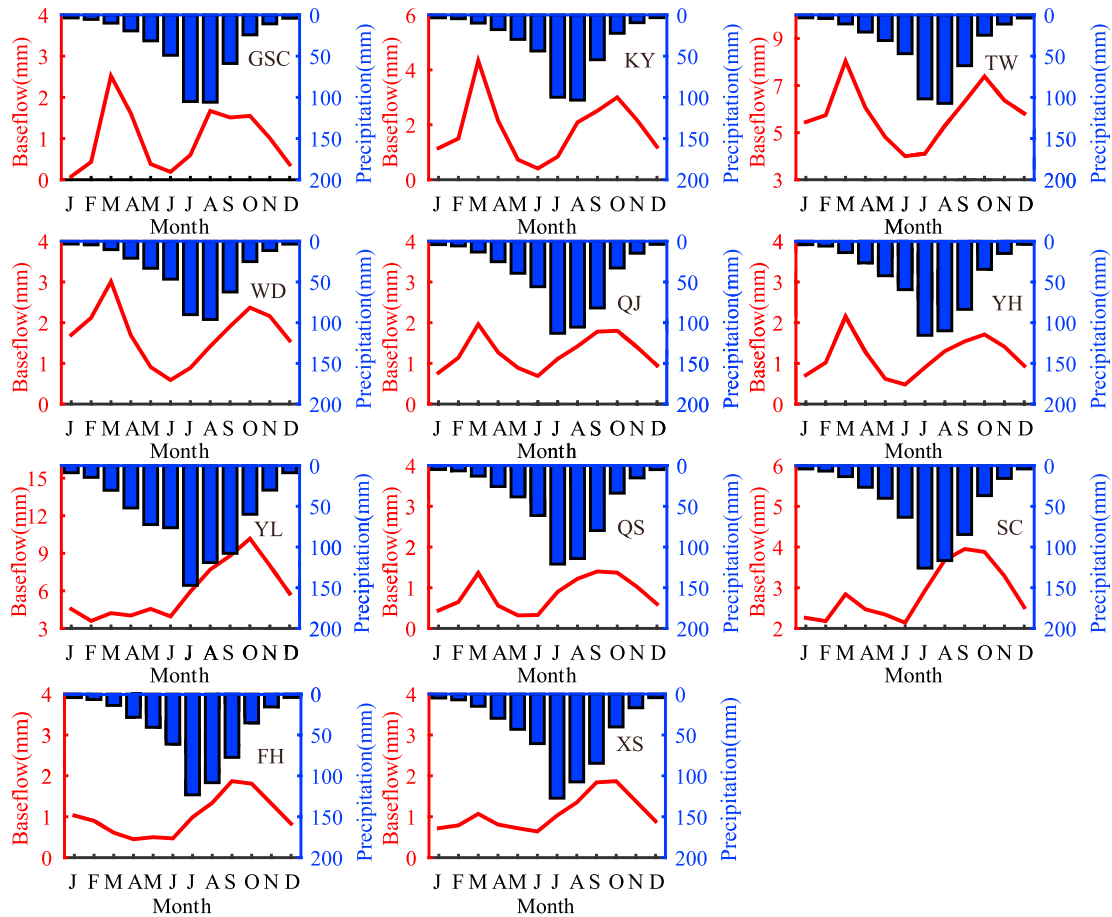


**Figure 6.** Spatial patterns of Mann-Kendall trends for seasonal baseflow index (*BFI*) in 11 basins of the Loess Plateau during the period 1961–2014.

greatest upward trend ( $p < 0.01$ ). In addition, the *BFI* was greater than 0.6 in the Tuwei, Wuding, and Sanchuan basins, with the highest *BFI* in Tuwei (0.73), indicating that streamflow in these basins is mainly supplied by baseflow. We attribute this large baseflow to the relatively large grassland and wind-sand areas that are characterized by a flat terrain and better vegetation cover, both of which are conducive to groundwater recharge (Qian et al., 2004). Thus, in these basins, groundwater resources are abundant, the water table is shallow, and the amount of water supplied to the river is large. However, basins with a lower *BFI* (e.g., Gushanchuan, Qiushui, and Sanchuan) generally are loess hilly areas, with incised gullies and satisfactory drainage conditions; these basins have a limited contribution to groundwater storage but are beneficial in forming surface runoff (Li et al., 2017).

We also investigated the annual mean *BFI* from 1961 to 1970, 1971 to 1999, and 2000 to 2014 (Figure 4). In contrast to baseflow, the annual mean *BFI* during the period 2000–2014 was greatest in all basins except Tuwei, Wuding, and Fenhe. We attribute this to the implementation of the Grain for Green program, which increased vegetation coverage, and resulted in a series of ecological effects, such as reduced surface runoff and enhanced precipitation infiltration. Increasing vegetation land cover is suggested to have decreased the water yield (1–48 mm/year) in about 38% of the Loess Plateau (Feng et al., 2012). Feng et al. (2010) found the permeation performance of most tree species exceeded that of natural grassland, and some species (i.e., sea-buckthorn and caragana) far exceeded the average level. In addition, vegetation can also change the soil structure and fortify soil permeability. Moreover and more important, during the period 2000–2014, the water consumption and evaporation are the greatest; the excessive water consumption and intense evaporation further reduce more surface runoff. In short, although streamflow significantly decreased, more water seeped into the soil and more surface runoff were consumed and evaporated, resulting in a relatively larger *BFI*.

**Table 3**  
Mann-Kendall Test and Multiyear Average BFI at Seasonal and Annual Scales for 11 Basins on the Loess Plateau From 1961 to 2014

Basin	BFI Z value					Mean BFI				
	MAM	JJA	SON	DJF	Annual	MAM	JJA	SON	DJF	Annual
GSC	3.29**	0.18	−0.16	4.55**	1.1	0.65	0.11	0.54	0.71	0.31
KY	0.56	−0.79	−1.22	1.1	1.5	0.57	0.15	0.61	0.72	0.42
TW	1.07	−2.36*	0.24	4.56**	1.12	0.81	0.5	0.81	0.85	0.73
WD	−1.84	−2.69**	−1.61	2.39*	−0.75	0.7	0.29	0.72	0.78	0.61
QJ	4.86**	3.46**	3.16**	5.63**	3.95**	0.7	0.2	0.62	0.82	0.43
YH	1.36	2.33*	1.58	4.8**	3.57**	0.65	0.18	0.6	0.77	0.42
YL	1.34	3.13*	0.37	−5.55**	0.96	0.63	0.45	0.63	0.81	0.58
QS	4.19**	2.02*	2.74**	3.39**	3.75**	0.6	0.13	0.6	0.8	0.33
SC	3.46**	3.94**	−0.54	5.42**	2.75**	0.86	0.48	0.8	0.93	0.7
FH	−4.43**	−0.39	−1.2	−2.35*	−0.93	0.49	0.33	0.64	0.75	0.55
XS	4.76**	2.41*	2.88**	6**	3.57**	0.72	0.25	0.65	0.84	0.49

Note. March–April–May (MAM), June–July–August (JJA), September–October–November (SON), and December–January–February (DJF) mean spring, summer, autumn, and winter, respectively. Acronyms are listed in Table 1. BFI, baseflow index.

\*\*Significance at the 99% level. \*Significance at the 95% level.

Trends in all basins for the seasonal *BFI* were more mixed and showed obvious spatial differences (Figure 6). In general, the *BFI* trended upward in all seasons for most basins except the Fenhe basin, which showed a downward trend during all seasons. In addition, the change to *BFI* was most significant in winter for all 11 basins. The relatively larger mean *BFI* in winter and spring indicates that baseflow is an important resource for maintaining streamflow in the dry season on the Loess Plateau (Table 3).

At the various time scales, therefore, the baseflow in all basins except Yanhe and Qingjian declined during the last five decades, whereas the *BFI* exhibited upward trends in most basins (Table 2 and Table 3). Although baseflow and observed streamflow decreased, basin characteristics were more conducive to water seepage into the ground, and compared to the decline in baseflow, the decline in surface runoff was more severe.

#### 4.3. Climate Elasticity Coefficient and Dynamic *n* at the Basin Scale

The mean climate elasticity coefficients of baseflow and *BFI* to precipitation and potential evapotranspiration at 11 basins during the period 1961–2014 are shown in Figure 7 and Table 4. For the baseflow, the multiyear mean  $\varepsilon_p$  (ranging from 0.14 [Tuwei] to 2.46 [Fenhe]) and  $\varepsilon_{E_0}$  (ranging from −2.56 [Qingjian] to −13.22 [Fenhe]) for the 11 basins were 1.22 and −7.43, respectively. This indicates that a 1% increase in multiyear mean precipitation (or multiyear mean potential evapotranspiration) would increase baseflow by 1.22% (or decrease baseflow by 7.43%). Climate elasticity of potential evapotranspiration was greater than that of precipitation, indicating a higher impact from potential evapotranspiration to baseflow variation than from precipitation. This is in contrast to their effect on surface runoff based on previous findings (Liang et al., 2015) that showed surface runoff variation was most sensitive to variations in precipitation (Berghuijs et al., 2017). Similarly, the *BFI* variations were most sensitive to variations in potential evapotranspiration; a 1% increase in multiyear mean potential evapotranspiration (or multiyear mean precipitation) would increase *BFI* variation by 1.66% (or decrease *BFI* variation by 0.22%; Table 4). We suggest that this is because potential evapotranspiration can reduce more runoff than baseflow and because implementation of soil and water conservation measures and reforestation have resulted in a more permeable soil (i.e., increased water seepage).

We estimated dynamic parameter *n* over the study period based on long-term mean annual runoff, precipitation, and potential evapotranspiration data (Table 4 and Figure S1). A higher *n* denotes higher actual evapotranspiration and lower runoff for a given precipitation and potential evapotranspiration (Liang et al., 2015). All basins except Yiluo showed upward trends, especially during the reforestation period (2000–2014), possibly because the implementation of the Grain for Green program changed the underlying surface properties of the basin (Hu et al., 2017). In addition, all basins except Yanhe showed steep increases during these three time periods (Table 4). Liang et al. (2015) found parameter *n* to have a positive relationship with

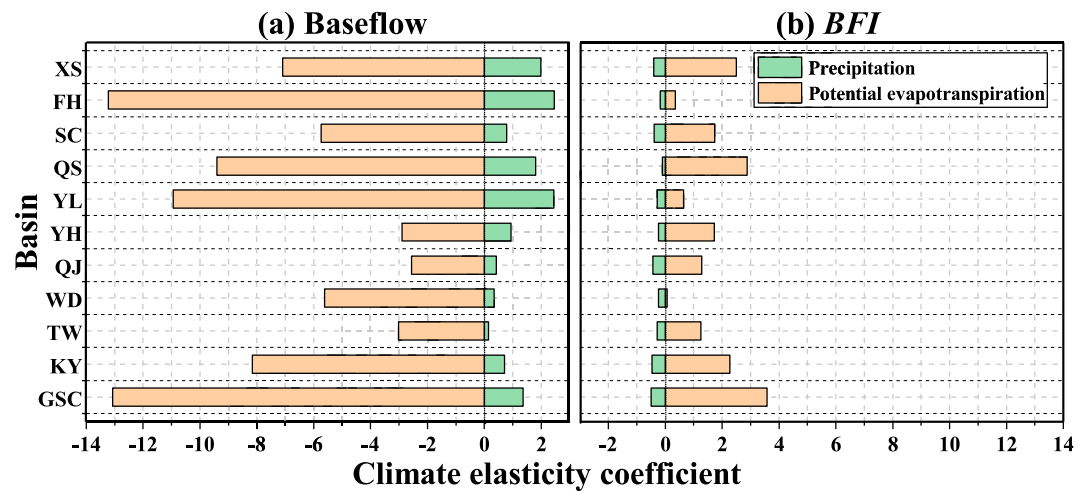


**Figure 7.** Climate elasticity coefficient to baseflow and baseflow index (*BFI*) in 11 basins of the Loess Plateau during the period 1961–2014. Acronyms on the y axis are listed in Table 1.

the percentage of affected area in the basin; this affected area has continued to increase during the last five decades, especially for slope measures. Moreover, the basin characteristics in Qiushui and Yiluo (or Gushanchuan and Kuye) changed the most, while the basin characteristics in Qingjian and Yanhe (or Yanhe and Yiluo) were not in evident for conservation engineering period (or for reforestation period; Table 4). We also investigated the relationship between parameter  $n$  and baseflow (Figure 8) and found a significant ( $p < 0.01$ ) negative correlation between baseflow and parameter  $n$  in all basins except Yanhe, for which the correlation was positive ( $p < 0.05$ ). Moreover, the negative correlations were stronger than that of the one basin with a positive relationship. Therefore, in general, an increase in parameter  $n$  could result in reduced baseflow for most area of the Loess Plateau.

#### 4.4. Attribution of Baseflow and *BFI* Variations

The relative contributions of climate variability and human activities to the decline in baseflow and *BFI* for the 11 study basins during the period 1961–2014 are shown in Figure 9. On average, human activities (73% and 76%) contributed more than climate variability (27% and 24%) to the baseflow decline for both the conservation engineering period (1971–1999) and the reforestation period (2000–2014), respectively. In nine basins (Gushanchuan, Kuye, Tuwei, Wuding, Yiluo, Qiushui, Sanchuan, Fenhe, and Xinshui), both climate variability and human activities caused a reduction in baseflow during the conservation engineering period

**Table 4**  
Climate Elasticity Coefficient and Dynamic  $n$  at Basin Scales for 11 Basins on the Loess Plateau From 1961 to 2014

Basin	Elasticity to baseflow		Elasticity to <i>BFI</i>		Dynamic $n$ value		
	$\epsilon_p$	$\epsilon_{E_0}$	$\epsilon_p$	$\epsilon_{E_0}$	BP	CEP	RFP
GSC	1.37	−13.07	−0.49	3.58	1.45	1.62	2.55
KY	0.71	−8.16	−0.47	2.28	1.26	1.39	2.16
TW	0.14	−3.02	−0.28	1.25	1.05	1.12	1.49
WD	0.34	−5.62	−0.24	0.06	1.65	1.74	2.03
QJ	0.42	−2.56	−0.44	1.29	2.07	2.06	2.41
YH	0.94	−2.9	−0.24	1.72	2.32	2.26	2.58
YL	2.45	−10.95	−0.29	0.65	1.61	2.11	2.26
QS	1.8	−9.41	−0.1	2.88	1.96	2.53	3.36
SC	0.78	−5.74	−0.39	1.74	1.88	2.22	2.80
FH	2.46	−13.22	−0.17	0.35	2.28	2.96	3.47
XS	1.98	−7.1	−0.41	2.5	2.66	2.84	3.37

Note. BF, CEP, and RFP denote the baseline period (1961–1970), “conservation engineering period” (1971–1999), and “reforestation period” (2000–2014), respectively

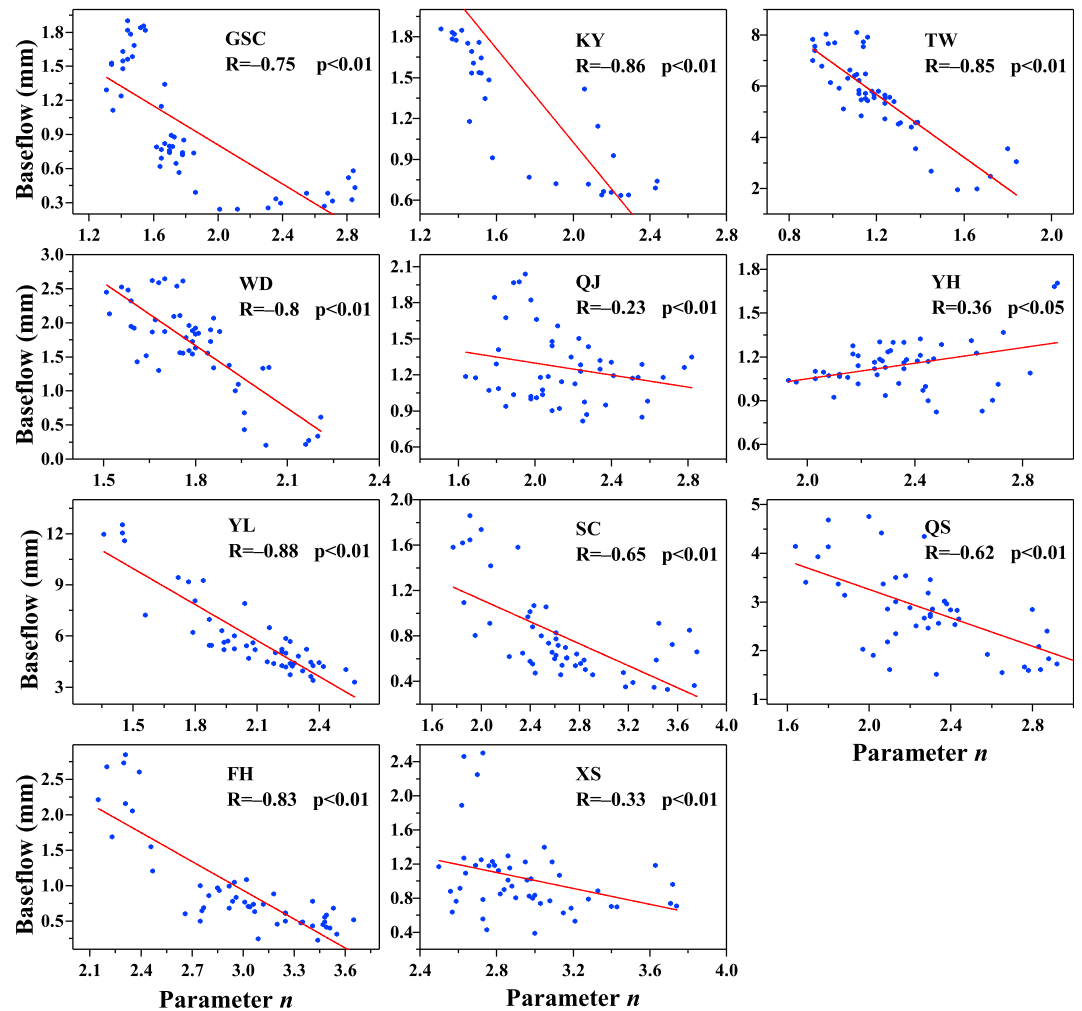


**Figure 8.** Relationship between baseflow and parameter  $n$  in 11 basins of the Loess Plateau. Acronyms are listed in Table 1.

and reforestation period, and human activities were identified as the major factor leading to the negative trends in the baseflow. In two basins (Qingjian and Yanhe), climate variability and human activities had opposing effects on baseflow variation, with climate variability reducing the baseflow and human activities increasing it. Furthermore, human activities had a greater impact on basins located in the northern and southern parts of the Loess Plateau, while climate variability played a major role in baseflow decline in the basins of the central plateau (Qingjian, Yanhe and Qiushui). Similar findings have been reported for the runoff (Liang et al., 2015).

The effect of climate variability (average 54%) on *BFI* variation was greater than the effect of human activities (−46%) during the conservation engineering period (Figure 9b), whereas they had the opposite effect. In eight basins (Gushanchuan, Kuye, Tuwei, Wuding, Yiluo, Qiushui, Fenhe, and Xinshui), climate variability increased the *BFI*, while human activities decreased it. In three basins (Qingjian, Yanhe, and Sanchuan), both climate variability and human activities increased the *BFI* value. During the reforestation period, the effect of climate variability (76%) on *BFI* variation was much greater than the effect of human activities (24%). On average, however, both climate variability and human activities could increase the *BFI*. For both the conservation engineering period and the reforestation period, climate variability increased the *BFI* in all basins, while human activities led to the opposite effects except for basins in the central area of the Loess Plateau (Qingjian and Yanhe). In general, for both baseflow and *BFI*, climate variability could lead to consistent variation in the 11 basins, whereas the effects of human activities in these basins varied.

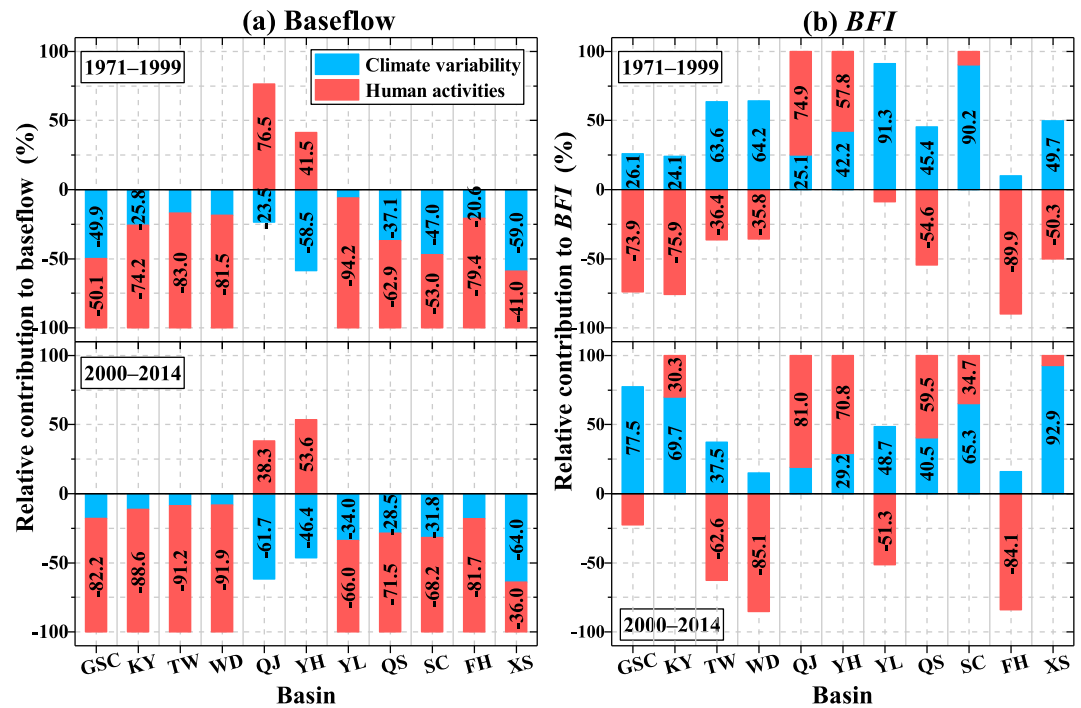


**Figure 9.** Relative contributions of climate variability and human activities to baseflow and baseflow index (*BFI*) variation in 11 basins of the Loess Plateau. Acronyms on the x axis are listed in Table 1.

#### 4.5. Underlying Explanation of Baseflow Variation

During the last five decades, the Loess Plateau (a representative semiarid region in China) has experienced an ongoing decline in runoff and a continuously decreasing trend in baseflow. Because the baseflow of the Loess Plateau accounts for a large proportion of total streamflow, ongoing decreases in baseflow can lead to a series of negative ecological effects, for example, exacerbating decreasing water levels in the Yellow River, which then leads to degraded river habitats, reduced lake area, and degeneration of epigenetic vegetation (Wang et al., 2008). Our findings showed human activities to be the major cause of reduced baseflow. These activities are principally the following: (1) excessive exploitation of groundwater, leading to a reduced lateral discharge of groundwater, that reduces the baseflow (Wang et al., 2006); (2) overgrazing, which reduces the baseflow by changing the underlying surface characteristics, which in turn induce a decrease in soil water retention capacity and water storage capacity and a change in the soil vegetation that significantly reduces the conservation function of the ground water resources (Hou et al., 2001), and the mining exploitation that can destroy the aquifer and result in loss of groundwater resources; and (3) excessive afforestation through large-scale soil and water conservation measures, such as the Grain for Green program, which has altered the hydrologic cycle with increased vegetation cover leading to increasing rates of actual evapotranspiration that intensifies soil desiccation (Zhang et al., 2018) and eventually reduces the baseflow. In general, however, groundwater exploitation has been the most active and principal driving factor to decrease the baseflow (Wang et al., 2008). In addition, climate variability is an indispensable factor driving reduced baseflow. The ongoing decreases in precipitation reduce the baseflow via decreased infiltration. Moreover, precipitation patterns have changed, with an increase in the frequency of high-intensity and extreme rainfall events. These lead to infiltration excess mode (Sun et al., 2015) and a consequent reduction in overall infiltration. Furthermore, increasing evapotranspiration rates resulting from higher temperatures can also reduce the baseflow. All of these climatic factors acting in concert have contributed to the diminished baseflow on the Loess Plateau.

Our study helps fill the gaps in our knowledge of baseflow variation and the causes of its variation in the Loess Plateau. Our findings will help policy makers implement reasonable water resources management policies and also provide valuable information for baseflow research in other semiarid regions all over the world.

## 5. Conclusion

Baseflow is a critical freshwater dry-season resource that plays an important role in the formation, maintenance, and recycle of runoff. It is important for maintaining river health, especially in water-limited semi-arid environments. In this study, the Loess Plateau was selected as a representative semiarid region to assess the impacts of climate variability and human activities on baseflow variation.

Our major findings are as follows:

1. The eight studied baseflow separation methods were found to provide consistent results during the low-flow period at both monthly and annual time scales. Some differences were apparent in the peak value of baseflow, with the results of the Bflow and Eckhardt filter methods providing higher values than those of the other methods.
2. The baseflow storage of all basins except Yanhe and Qingjian at the various time scales have declined over the last five decades, whereas the *BFI* has exhibited upward trends in most basins. In addition, the baseflow has contributed greatly to total streamflow on the Loess Plateau.
3. Both baseflow and *BFI* variations were more sensitive to variations in potential evapotranspiration than precipitation. A 1% increase in precipitation would result in 1.22% increase in baseflow and 0.22% decrease in *BFI*, whereas a 1% increase in potential evapotranspiration would result in a 7.43% decrease in baseflow and 1.66% increase in *BFI*. The parameter *n* showed an upward trend over the study period; an increasing *n* suggests that baseflow storage could decrease for most of the Loess Plateau.
4. Human activities have played the dominant role in baseflow variation, whereas climate variability has been the main factor to alter the *BFI*. Human activities contributed more to baseflow decline on average for both the conservation engineering period (73%), which extended from 1971 to 1999, and the reforestation period (76%), which was from 2000 to 2014. The contributions of climate variability and human activities to *BFI* variations during the conservation engineering period were 54% and -46%, respectively, and were 76% and 24%, respectively during the reforestation period.

## Acknowledgments

This research was supported by the National Natural Science Foundation of China (41622101 and 41877155), the National Key Research and Development Program of China (2016YFC0501604), Beijing Higher Education Young Elite Teacher Project, and State Key Laboratory of Earth Surface Processes and Resource Ecology. We are grateful to the Yellow River Conservancy Commission (YRCC) for providing the monthly runoff (<http://www.yellowriver.gov.cn/other/hhgb/>) and China Meteorological Administration (CMA) for providing the climate data sets (<http://data.cma.cn/>).

## References

- Ahiablame, L., Sheshukov, A. Y., Rahmani, V., & Moriasi, D. (2017). Annual baseflow variations as influenced by climate variability and agricultural land use change in the Missouri River Basin. *Journal of Hydrology*, *551*, 188–202. <https://doi.org/10.1016/j.jhydrol.2017.05.055>
- Arnold, J. G., & Allen, P. M. (1999). Automated methods for estimating baseflow and ground water recharge from streamflow records. *Journal of the American Water Resources Association*, *35*(2), 411–424. <https://doi.org/10.1111/j.1752-1688.1999.tb03599.x>
- Barlow, P. M., Cunningham, W. L., Zhai, T., & Gray, M. (2017). Geological Survey Groundwater Toolbox version 1.3.1, a graphical and mapping interface for analysis of hydrologic data, U.S. Geological Survey Software Release, 26 May 2017. <https://doi.org/10.5066/F5067R5078C5069G>
- Berghuijs, W. R., Larsen, J. R., van Emmerik, T. H. M., & Woods, R. A. (2017). A global assessment of runoff sensitivity to changes in precipitation, potential evaporation, and other factors. *Water Resources Research*, *53*, 8475–8486. <https://doi.org/10.1002/2017wr021593>
- Brutsaert, W. (2005). *Hydrology: An introduction* (p. 605). Cambridge, UK: Cambridge University Press. <https://doi.org/10.1017/CBO9780511808470>
- Budyko, M. I. (1974). *Climate and Life*. New York, CA: Academic Press.
- Choudhury, B. J. (1999). Evaluation of an empirical equation for annual evaporation using field observations and results from a biophysical model. *Journal of Hydrology*, *216*(1–2), 99–110. [https://doi.org/10.1016/S0022-1694\(98\)00293-5](https://doi.org/10.1016/S0022-1694(98)00293-5)
- Christine, A. R., Matthew, P. M., Susong, D. D., Tillman, F. D., & David, W. A. (2015). Regional scale estimates of baseflow and factors influencing baseflow in the Upper Colorado River Basin. *Journal of Hydrology: Regional Studies*, *4*, 91–107.
- Eckhardt, K. (2005). How to construct recursive digital filters for baseflow separation. *Hydrological Processes*, *19*(2), 507–515. <https://doi.org/10.1002/hyp.5675>
- Eckhardt, K. (2008). A comparison of baseflow indices, which were calculated with seven different baseflow separation methods. *Journal of Hydrology*, *352*(1–2), 168–173. <https://doi.org/10.1016/j.jhydrol.2008.01.005>
- Fan, Y. T., Chen, Y. N., Liu, Y. B., & Li, W. H. (2013). Variation of baseflows in the headstreams of the Tarim River Basin during 1960–2007. *Journal of Hydrology*, *487*, 98–108. <https://doi.org/10.1016/j.jhydrol.2013.02.037>
- Feng, X. M., Sun, G., Fu, B. J., Su, C. H., Liu, Y., & Lamparski, H. (2012). Regional effects of vegetation restoration on water yield across the Loess Plateau, China. *Hydrology and Earth System Sciences*, *16*(8), 2617–2628. <https://doi.org/10.5194/hess-16-2617-2012>
- Feng, X. M., Wang, Y. F., Chen, L. D., Fu, B. J., & Bai, G. S. (2010). Modeling soil erosion and its response to land-use change in hilly catchments of the Chinese Loess Plateau. *Geomorphology*, *118*(3–4), 239–248. <https://doi.org/10.1016/j.geomorph.2010.01.004>
- Ficklin, D. L., Robeson, S. M., & Knouft, J. H. (2016). Impacts of recent climate change on trends in baseflow and stormflow in United States watersheds. *Geophysical Research Letters*, *43*, 5079–5088. <https://doi.org/10.1002/2016gl069121>
- Fu, B. J., Liu, Y., Lu, Y. H., He, C. S., Zeng, Y., & Wu, B. F. (2011). Assessing the soil erosion control service of ecosystems change in the Loess Plateau of China. *Ecological Complexity*, *8*(4), 284–293. <https://doi.org/10.1016/j.ecocom.2011.07.003>
- Fu, B. J., Wang, S., Liu, Y., Liu, J. B., Liang, W., & Miao, C. Y. (2017). Hydrogeomorphic ecosystem responses to natural and anthropogenic changes in the Loess Plateau of China. *Annual Review of Earth and Planetary Sciences*, *45*(1), 223–243. <https://doi.org/10.1146/annurev-earth-063016-020552>

- Gao, G. Y., Fu, B. J., Wang, S., Liang, W., & Jiang, X. H. (2016). Determining the hydrological responses to climate variability and land use/cover change in the Loess Plateau with the Budyko framework. *Science of the Total Environment*, 557–558, 331–342. <https://doi.org/10.1016/j.scitotenv.2016.03.019>
- Hargreaves, G. H., & Samani, A. (1985). Reference crop evapotranspiration from temperature. *Applied Engineering in Agriculture*, 1(2), 96–99. <https://doi.org/10.13031/2013.26773>
- Harman, C., & Sivapalan, M. (2009). A similarity framework to assess controls on shallow subsurface flow dynamics in hillslopes. *Water Resources Research*, 45, W01417. <https://doi.org/10.1029/2008WR007067>
- Hou, C. M., Zhang, Z. Q., & Liu, X. W. (2001). Eco-environmental problem in Yellow River sources region and corresponding solutions in sustainable development. *China Population, Resources and Environment*, 11, 51–53.
- Hu, J., Lu, Y. H., Fu, B. J., Comber, A. J., & Harris, P. (2017). Quantifying the effect of ecological restoration on runoff and sediment yields: A meta-analysis for the Loess Plateau of China. *Progress in Physical Geography*, 41(6), 753–774. <https://doi.org/10.1177/0309133317738710>
- Huang, J. P., Ji, M. X., Xie, Y. K., Wang, S. S., He, Y. L., & Ran, J. J. (2016). Global semi-arid climate change over last 60 years. *Climate Dynamics*, 46(3–4), 1131–1150. <https://doi.org/10.1007/s00382-015-2636-8>
- Juckem, P. F., Hunt, R. J., Anderson, M. P., & Robertson, D. M. (2008). Effects of climate and land management change on streamflow in the driftless area of Wisconsin. *Journal of Hydrology*, 355(1–4), 123–130. <https://doi.org/10.1016/j.jhydrol.2008.03.010>
- Kendall, M. G. (1975). *Rank Correlation Methods*. London: Griffin.
- Kong, D. X., Miao, C. Y., Wu, J. W., & Duan, Q. Y. (2016). Impact assessment of climate change and human activities on net runoff in the Yellow River Basin from 1951 to 2012. *Ecological Engineering*, 91, 566–573. <https://doi.org/10.1016/j.ecoleng.2016.02.023>
- Li, H. J., Liu, H. J., & Zhang, Z. J. (2018). Analysis in water demand and irrigation of main crop in Fenhe irrigation area. *Shanxi Water Resources*, 34(10), 7–9.
- Li, Q., Wei, X. H., Zhang, M. F., Liu, W. F., Giles-Hansen, K., & Wang, Y. (2018). The cumulative effects of forest disturbance and climate variability on streamflow components in a large forest-dominated watershed. *Journal of Hydrology*, 557, 448–459. <https://doi.org/10.1016/j.jhydrol.2017.12.056>
- Li, Z., Lin, X. Q., Xiang, W., Chen, X., & Huang, T. M. (2017). Stable isotope tracing of headwater sources in a river on China's Loess Plateau. *Hydrological Sciences Journal*, 62(13), 2150–2159. <https://doi.org/10.1080/02626667.2017.1368519>
- Liang, W., Bai, D., Wang, F. Y., Fu, B. J., Yan, J. P., Wang, S., et al. (2015). Quantifying the impacts of climate change and ecological restoration on streamflow changes based on a Budyko hydrological model in China's Loess Plateau. *Water Resources Research*, 51, 6500–6519. <https://doi.org/10.1002/2014wr016589>
- Linsley, R. K., Kohler, M. A., & Paulhus, J. L. H. (1975). *Hydrology for engineers*. New York: McGraw-Hill.
- Liu, M. X., Xu, X. L., Xu, C. H., Sun, A. Y., Wang, K. L., Scanlon, B. R., & Zhang, L. (2017). A new drought index that considers the joint effects of climate and land surface change. *Water Resources Research*, 53, 3262–3278. <https://doi.org/10.1002/2016wr020178>
- Liu, Z. P., Shao, M. A., & Wang, Y. Q. (2012). Large-scale spatial variability and distribution of soil organic carbon across the entire Loess Plateau, China. *Soil Research*, 50(2), 114–124. <https://doi.org/10.1017/Sr11183>
- Lyne, V., & Hollick, M. (1979). Stochastic time-variable rainfall-runoff modeling (pp. 89–93.). Conference: Aust. Natl. Conf. Publ. At: Perth, Australia.
- Miao, C. Y., Ni, J. R., Borthwick, A. G. L., & Yang, L. (2011). A preliminary estimate of human and natural contributions to the changes in water discharge and sediment load in the Yellow River. *Global and Planetary Change*, 76(3–4), 196–205. <https://doi.org/10.1016/j.gloplacha.2011.01.008>
- Mwakalila, S., Feyen, J., & Wyseure, G. (2002). The influence of physical catchment properties on baseflow in semi-arid environments. *Journal of Arid Environments*, 52(2), 245–258. <https://doi.org/10.1006/jare.2001.0947>
- Nathan, R. J., & McMahon, T. A. (1990). Evaluation of automated techniques for base-flow and recession analyses. *Water Resources Research*, 26(7), 1465–1473. <https://doi.org/10.1029/WR026i007p01465>
- Partington, D., Brunner, P., Simmons, C. T., Werner, A. D., Therrien, R., Maier, H. R., & Dandy, G. C. (2012). Evaluation of outputs from automated baseflow separation methods against simulated baseflow from a physically based, surface water-groundwater flow model. *Journal of Hydrology*, 458–459, 28–39. <https://doi.org/10.1016/j.jhydrol.2012.06.029>
- Price, K. (2011). Effects of watershed topography, soils, land use, and climate on baseflow hydrology in humid regions: A review. *Progress in Physical Geography*, 35(4), 465–492. <https://doi.org/10.1177/0309133311402714>
- Qian, Y. P., Jiang, X. H., Jin, S. Y., & Zhang, P. D. (2004). Analysis on the characteristic and variation of base flow in loessial plateau of the middle reaches of Huanghe River. *Journal of Earth Sciences and Environment*, 26(2), 88–91.
- Rutledge, A. T. (1998). Computer programs for describing the recession of ground-water discharge and for estimating mean ground-water recharge and discharge from streamflow records—Update, U.S. Geological Survey Water-Resources Investigations Report 98–4148, 43, <http://pubs.usgs.gov/wri/wri984148/>.
- Schaake, J. C. (1990). From climate to flow. In P. E. Waggoner (Ed.), *Climate change and U.S. water resources* (Vol. 8, pp. 177–206). New York: John Wiley.
- Seager, R., Naik, N., & Vecchi, G. A. (2010). Thermodynamic and dynamic mechanisms for large-scale changes in the hydrological cycle in response to global warming. *Journal of Climate*, 23(17), 4651–4668. <https://doi.org/10.1175/2010jcli3655.1>
- Sloto, R. A., and Crouse, M. Y. (1996). HYSEP—A computer program for streamflow hydrograph separation and analysis, U.S. Geological Survey Water-Resources Investigations Report 96–4040 (46 pp.). Retrieved from <http://pubs.er.usgs.gov/publication/wri964040>
- Spongberg, M. E. (2000). Spectral analysis of base flow separation with digital filters. *Water Resources Research*, 36(3), 745–752. <https://doi.org/10.1029/1999WR900303>
- Standish-Lee, P., Loboschewsky, E., & Beuhler, M. (2005). The future of water: Identifying and developing effective methods for managing water in arid and semi-arid regions. Sacramento, CA: Black & Veatch.
- Sun, Q. H., Miao, C. Y., Duan, Q. Y., & Wang, Y. F. (2015). Temperature and precipitation changes over the Loess Plateau between 1961 and 2011, based on high-density gauge observations. *Global and Planetary Change*, 132, 1–10. <https://doi.org/10.1016/j.gloplacha.2015.05.011>
- Tallaksen, L. M. (1995). A review of baseflow recession analysis. *Journal of Hydrology*, 165(1–4), 349–370. [https://doi.org/10.1016/0022-1694\(95\)92779-D](https://doi.org/10.1016/0022-1694(95)92779-D)
- Tetzlaff, D., & Soulsby, C. (2008). Sources of baseflow in larger catchments—Using tracers to develop a holistic understanding of runoff generation. *Journal of Hydrology*, 359(3–4), 287–302. <https://doi.org/10.1016/j.jhydrol.2008.07.008>
- Wahl, K. L., & Wahl, T. L. (1995). Determining the flow of Comal Springs at New Braunfels, Texas. In *Proceedings of Texas Water 95* (pp. 77–86). San Antonio, TX: American Society of Civil Engineers.

- Wang, G. Q., Zhang, J. Y., Xuan, Y. Q., Liu, J. F., Jin, J. L. Z., Bao, X., et al. (2013). Simulating the impact of climate change on runoff in a typical river catchment of the Loess Plateau, China. *Journal of Hydrometeorology*, *14*(5), 1553–1561. <https://doi.org/10.1175/Jhm-D-12-081.1>
- Wang, W. K., Wang, Y. L., & Duan, L. (2006). Groundwater environment evaluation and renew ability measure in the Guanzhong basin. Zhengzhou, China: Huanghe Water Resource Publishing Press.
- Wang, Y. L., Wang, W. K., Qian, Y. P., Duan, L., & Yang, Z. Y. (2008). Change characteristics and driving forces of base flow of Yellow River. *Journal of Natural Resources*, *23*(3), 479–486.
- Ward, R. C., & Robinson, M. (1990). *Principles of hydrology* (p. 365). Maidenhead: McGraw Hill.
- Wu, J. W., Miao, C. Y., Tang, X., Duan, Q. Y., & He, X. J. (2018). A nonparametric standardized runoff index for characterizing hydrological drought on the Loess Plateau, China. *Global and Planetary Change*, *161*, 53–65. <https://doi.org/10.1016/j.gloplacha.2017.12.006>
- Wu, J. W., Miao, C. Y., Wang, Y. M., Duan, Q. Y., & Zhang, X. M. (2017). Contribution analysis of the long-term changes in seasonal runoff on the Loess Plateau, China, using eight Budyko-based methods. *Journal of Hydrology*, *545*, 263–275. <https://doi.org/10.1016/j.jhydrol.2016.12.050>
- Wu, J. W., Miao, C. Y., Zheng, H. Y., Duan, Q. Y., Lei, X. H., & Li, H. (2018). Meteorological and hydrological drought on the Loess Plateau, China: Evolutionary characteristics, impact, and propagation. *Journal of Geophysical Research: Atmospheres*, *123*, 11,569–11,584. <https://doi.org/10.1029/2018JD029145>
- Xu, L. L., Liu, J. L., Jin, C. J., Wang, A. Z., Guan, D. X., Wu, J. B., & Yuan, F. H. (2011). Baseflow separation methods in hydrological process research: A review. *Chinese Journal of Applied Ecology*, *22*(11), 3073–3080.
- Xu, R., Wang, X., & Zheng, W. (2016). Research progresses in baseflow separation methods. *Bulletin of Soil and Water Conservation*, *36*(5), 352–359.
- Xu, X. L., Scanlon, B. R., Schilling, K., & Sun, A. (2013). Relative importance of climate and land surface changes on hydrologic changes in the US Midwest since the 1930s: Implications for biofuel production. *Journal of Hydrology*, *497*, 110–120. <https://doi.org/10.1016/j.jhydrol.2013.05.041>
- Yang, H. B., Yang, D. W., Lei, Z. D., & Sun, F. B. (2008). New analytical derivation of the mean annual water-energy balance equation. *Water Resources Research*, *44*, W03410. <https://doi.org/10.1029/2007WR006135>
- Yang, Y., Jia, X., Wendroth, O., Liu, B., Shi, Y., Huang, T., & Bai, X. (2019). Noise-assisted multivariate empirical mode decomposition of saturated hydraulic conductivity along a south-north transect across the Loess Plateau of China. *Soil Science Society of America Journal*. <https://doi.org/10.2136/sssaj2018.11.0438>
- Yang, Y., Wang, L., Wendroth, O., Liu, B., Cheng, C., Huang, T., & Shi, Y. (2019). Is the laser diffraction method reliable for soil particle size distribution analysis? An evaluation by sieve-pipette method and scanning electron microscopy. *Soil Science Society of America Journal*. <https://doi.org/10.2136/sssaj2018.07.0252>
- Yue, S., Pilon, P., & Cavadias, G. (2002). Power of the Mann-Kendall and Spearman's rho tests for detecting monotonic trends in hydrological series. *Journal of Hydrology*, *259*(1–4), 254–271. [https://doi.org/10.1016/S0022-1694\(01\)00594-7](https://doi.org/10.1016/S0022-1694(01)00594-7)
- Zhang, Q., Liu, J. Y., Singh, V. P., Gu, X. H., & Chen, X. H. (2016). Evaluation of impacts of climate change and human activities on streamflow in the Poyang Lake basin, China. *Hydrological Processes*, *30*(14), 2562–2576. <https://doi.org/10.1002/hyp.10814>
- Zhang, Q., Sun, P., Chen, X. H., & Jiang, T. (2011). Hydrological extremes in the Poyang Lake basin, China: Changing properties, causes and impacts. *Hydrological Processes*, *25*(20), 3121–3130. <https://doi.org/10.1002/hyp.8031>
- Zhang, S. L., Yang, D. W., Yang, Y. T., Piao, S. L., Yang, H. B., Lei, H. M., & Fu, B. J. (2018). Excessive afforestation and soil drying on China's Loess Plateau. *Journal of Geophysical Research: Biogeosciences*, *123*(3), 923–935. <https://doi.org/10.1002/2017JG004038>
- Zheng, H. X., Zhang, L., Zhu, R. R., Liu, C. M., Sato, Y., & Fukushima, Y. (2009). Responses of streamflow to climate and land surface change in the headwaters of the Yellow River Basin. *Water Resources Research*, *45*, W00A19. <https://doi.org/10.1029/2007WR006665>
- Zhou, S., Yu, B. F., Huang, Y. F., & Wang, G. Q. (2015). The complementary relationship and generation of the Budyko functions. *Geophysical Research Letters*, *42*, 1781–1790. <https://doi.org/10.1002/2015gl063511>
- Zhou, X., Shen, C., Ni, G. H., & Hu, H. C. (2017). Digital filter baseflow separation method based on a master recession curve. *Journal of Tsinghua University (Science and Technology)*, *57*(3), 318–323.
- Zomlot, Z., Verbeiren, B., Huysmans, M., & Batelaan, O. (2015). Spatial distribution of groundwater recharge and base flow: Assessment of controlling factors. *Journal of Hydrology: Regional Studies*, *4*, 349–368.